



## Supplementary Information for

REM sleep's unique associations with corticosterone regulation, apoptotic pathways and behavior in chronic stress in mice

Mathieu Nollet, Harriet Hicks, Andrew P. McCarthy, Huihai Wu, Carla S. Möller-Levet, Emma E. Laing, Karim Malki, Nathan Lawless, Keith A. Wafford, Derk-Jan Dijk, Raphaelle Winsky-Sommerer

Derk-Jan Dijk  
Email: [d.j.dijk@surrey.ac.uk](mailto:d.j.dijk@surrey.ac.uk)

Raphaelle Winsky-Sommerer  
Email: [r.winsky-sommerer@surrey.ac.uk](mailto:r.winsky-sommerer@surrey.ac.uk)

### **This PDF file includes:**

SI Materials and Methods  
Figs. S1 to S9  
Table S1  
References for SI reference citations

### **Other supplementary materials for this manuscript include the following:**

Datasets S1 to S9

## SI Materials and Methods

### Procedures to reduce bias

The study was conducted with baseline assessments, and as a between-group design (UCMS *versus* control) with random assignment to treatment groups. Based on previous studies in which variables relevant to this study were assessed (i.e., physical and behavioral parameters) (1, 2), a sample size of  $n = 9$  per study arm (i.e., two treatments) was chosen. This sample size yields 80% power to detect a difference (2-sided test  $P < 0.05$ ) of 20% in behavioral despair assessed by the forced swim test. Behavioral tests were video-recorded and all scored offline by two experimenters blind to treatment. Scoring agreement among raters was assessed using Kendall's coefficient of concordance  $W$  computed in R using the `irr` package (<https://cran.r-project.org/web/packages/irr/index.html>). The coat state, grooming test and nest building test were scored 'online' by two experimenters, one blind to treatment (65% of data double-scored). Very high to complete concordance between scorers was reached with Kendall's coefficients of concordance  $W$  ranging between 0.92 ( $P = 2.4 \times 10^{-6}$ ) and 1 ( $P = 8.4 \times 10^{-3}$ ). Automated scoring of EEG/electromyogram (EMG) data was confirmed by visual inspection of all files by an experimenter blind to treatment, and visual scoring for baseline, days #15 and #36 (% NREM sleep: Kendall's coefficient of concordance  $W = 0.991$ ,  $P = 6.54 \times 10^{-8}$ ; % REM sleep: Kendall's  $W = 0.989$ ,  $P = 7.11 \times 10^{-8}$ ; % Waking: Kendall's  $W = 0.989$ ,  $P = 6.90 \times 10^{-8}$ ). RNA sequencing analyses were performed by two bioinformatics teams (i.e., Eli Lilly and University of Surrey).

Data attrition occurred for the forced swim test ( $n = 8$  per group; test stopped by the experimenter), sleep data ( $n = 8$  per group: two subjects excluded due to EEG/EMG artefacts precluding scoring), the dexamethasone suppression test ( $n = 5-8$  per group due to limitations during blood collection) and RNA sequencing ( $n = 7-9$  per group due to issues during tissue collection). Further methods to reduce bias and risk of false discovery are discussed in the Statistics section.

### Housing conditions and Surgery

Mice were housed in groups prior to the start of the experiment, under a 12-h light/dark cycle, controlled ambient temperature (20-22°C) and relative humidity ( $55 \pm 10\%$ ) with food and water *ad libitum*. After 7 days of acclimatization, mice aged  $12.4 \pm 1.4$  (Mean  $\pm$  SD) weeks were implanted with a telemetry transmitter (TL11M2-F20-EET, Data Sciences International, St. Paul, MN, USA) connected to electrodes for continuous EEG/EMG recordings. Under anesthesia (isoflurane; induction 3-4%, maintenance 2-2.5% with progressive decreasing), two stainless-steel EEG electrodes (length of screw shaft: 2.4 mm; head diameter: 2.16 mm; shaft diameter: 1.19 mm; Plastics One, Roanoke, VA, USA) were implanted epidurally over the right frontal and parietal cortices, as previously described (3). The electrodes were connected to the telemetry transmitter via medical-grade stainless-steel wires. The EEG electrodes were covered with dental cement (Kemdent, Purton, Swindon, UK). Two EMG stainless-steel leads were inserted into the neck muscles  $\sim 5$  mm apart and sutured into place. The telemetry transmitter was placed in a subcutaneous pocket and positioned along the left-dorsal flank. Analgesia was administered at the onset of the surgery (Vetergesic, 0.1 mg/kg, subcutaneous injection). Animals were allowed to recover for  $5.6 \pm 1.4$  weeks (Mean  $\pm$  SD).

### Experimental setup

After surgery, animals were allowed to recover for  $5.6 \pm 1.4$  weeks (Mean  $\pm$  SD). During recovery, mice were singly housed and randomly assigned to the control and the UCMS groups ( $n = 9$  mice per group), housed in two separate rooms. Home cages were placed in ventilated cabinets with a light intensity of  $200 \pm 13.4$  mW/m<sup>2</sup> ( $\sim 60$  lux) at the level of the cage bottom during the light period

with a 12-h light-dark cycle. Nesting material (bedding) was provided during one week after the surgery to aid thermoregulation, but was removed to avoid any bias with the nest building test performed during the UCMS paradigm. Cardboard play tunnels were also placed into home cages. Baseline data collection started when the mice were 18 weeks of age with baseline measurements, before the start of the UCMS protocol.

### **Unpredictable chronic mild stress (UCMS) paradigm**

The stress paradigm has been extensively used in the context of neurobiological mechanisms underlying stress, depression and the effects of antidepressants (4). The paradigm used in the study on BALB/c mice is a variant of procedures developed by Willner and collaborators in rats (5). The use of BALB/c mice has been shown to be relevant for the study of stress- and mood-related disorders. Compared to other inbred strains, BALB/c mice display high susceptibility to anxiety (6) and chronic stress (7), and are also responsive to antidepressant treatments (8-10). Briefly, mice were daily subjected to various socio-environmental low intensity stressors (social stress, cage tilting, confinement stress, cage without sawdust, soiled sawdust, damp sawdust, sawdust change, water stress and predator [rat] odor) according to an unpredictable schedule for nine weeks (*SI Appendix*, Table S1). The stressors used in our study are considered mild and more severe stressors such as food or water deprivation, cold water immersion or footshock (4) were not used. Nevertheless, the UCMS paradigm induces a depressive-like phenotype of moderate severity. No stressor was applied during the light period.

### **Physical assessments**

Body weight and coat state were assessed weekly and twice a week, respectively, as markers of the progression of the UCMS-evoked syndrome (5). The coat state represents an indirect evaluation of the grooming behavior, an index of self-care behavior, and was evaluated by giving a score (0 = well-groomed, 0.5 = moderate degradation, 1 = unkempt) to the coat on seven body parts (i.e., head, neck, dorsal area, ventral area, tail, front and hind paws, and genital area). The total score resulted from the sum of scores, with a higher score indicating that the coat is in poor condition. Baseline values of the coat state and the body weight were assessed 3 days before the beginning of the UCMS paradigm.

### **Corticosterone regulation: dexamethasone suppression test**

To assess the effects of UCMS on the HPA axis negative feedback and corticosterone regulation, the dexamethasone (DEX) suppression test was used. All mice were administered intraperitoneally the glucocorticoid receptor agonist dexamethasone-phosphate (DEX; D-1159, Sigma-Aldrich, St. Louis, MO, USA; 0.1 mg/kg in 0.9% NaCl) and saline (0.9% NaCl), 24-h apart in a crossover design. All injections were performed between ZT12 and ZT13 when plasma corticosterone levels are high (11). Two hours after the injection, blood was collected through the submandibular vein (12) in EDTA-coated tubes. Blood samples were quickly centrifuged at 2000g and plasma was collected and stored at -20°C. Corticosterone levels were assessed using a <sup>125</sup>I-labeled corticosterone double-antibody radioimmunoassay kit (MP Biomedicals, New York, NY, USA) according to the manufacturer's protocol. The percentage of corticosterone suppression induced by DEX administration was calculated by the ratio between basal corticosterone levels (assessed after the saline injection) and the corticosterone levels after DEX injection using the following formula:

$$\text{Percentage of [CORT] suppression} = 100 - \frac{[\text{CORT}] \text{ after DEX} \times 100}{[\text{CORT}] \text{ after saline}}$$

## EEG/EMG recordings and scoring

Telemetry transmitters were activated thirty minutes before each recording session (day -6 for baseline; UCMS: day #3, 8, 15, 22, 29, 36, 55 and 64). EEG/EMG signals were recorded continuously for 48-h using Data Sciences International hardware and Dataquest ART software (Data Sciences International, St. Paul, MN, USA). The EEG and EMG data were transmitted at 455 kHz to an RPC-1 receiver (Data Science International) and sampled at 250 Hz and filtered with a high-pass (3 dB, 0.5 Hz) and a low-pass, anti-aliasing (50 Hz) analog filter. The data analyzed consisted of 24-h recordings starting at dark onset (ZT12). Vigilance states were determined using SCORE-2004™, an automated sleep scoring system based on an updated version of the real-time sleep/wake monitoring system SCORE™ (13). Raw EEG and EMG signals were resampled at 100 and 71.4 Hz respectively using Matlab 2016a (MathWorks, Natick, MA, USA). The process of assigning a state of wakefulness, NREMS or REMS consisted of first extracting four features from the 10-s EEG epoch; amplitude, zero-crossings (a measure of EEG frequency), harmonic amplitude and harmonic frequency. A mean of the integrated EMG over the 10-s epoch were also used in arousal state assignment. Unique templates were then generated from these parameters through a user-dependent teaching process allowing the state scoring procedure (14). The time spent in NREMS and REMS was expressed as a percentage of total sleep time in the 12-h recording time for the light and dark periods.

## EEG power density

EEG power spectra were computed for consecutive 10-s epochs by a fast Fourier transform (frequency range: 0.1–20 Hz; resolution: 0.1 Hz; non-overlapping Hanning window). For the mice included in spectral analyses ( $n = 8$  per group), epochs containing EEG artifacts were discarded from EEG spectral analyses (% of recording time:  $7.9 \pm 0.8\%$ ). EEG power spectra were determined for NREMS, REMS, and wakefulness during the 12-h light and dark periods. EEG power spectra are expressed as a percentage of total EEG power (frequency range: 1-20 Hz; resolution: 1 Hz). EEG delta power during NREMS and EEG theta power during REMS were computed by adding the EEG power in the frequencies ranging from 1 to 4.5 Hz and from 6 to 9 Hz, respectively. Mean values were individually normalized to the mean total power in NREMS and REMS.

## Behavioral testing

All behavioral tests were performed between Zeitgeber time (ZT) 13 and ZT17 (i.e., during the dark, active phase) under red light, with a maximum of one test per day.

**Grooming test (GT).** The GT provides an evaluation of the grooming behavior, an index of self-centered behavior (5). Mice were placed in a temporary cage to be briefly sprayed with a 10% sucrose solution on their dorsal coat and were then immediately placed back in their home cage. The latency of the first grooming behavior, as well as the total grooming duration, were recorded over 5 min. The test was performed weekly during the first five weeks of UCMS (days #10, 17, 24, 31 and 38 with a prior baseline test performed 3 days before the beginning of the UCMS paradigm).

**Nest building test (NBT).** The NBT assesses the motivation to build a nest (5). One hour before the beginning of the dark phase (ZT11), a cotton nestlet (5x5 cm, 2-3 g; LBS Biotechnology, Hookwood, UK) was placed in the home cage. Twenty-four hours after the introduction of the cotton nestlet, nest building was evaluated according to the 5-score scale (15). No stressor was applied during the 24 hours of the NBT. The test was performed weekly during the first five weeks of UCMS (days #9, 16, 23, 30 and 37; baseline measurements were performed four days before the beginning of the UCMS paradigm).

**Social novelty preference test (SNP).** The SNP test was used to assess social behavior and was conducted as previously described (16). The test consisted of three phases. The mouse was first

placed into the middle chamber of an interconnected three-chambered box (60 cm length x 30 cm wide x 30 cm high). During this habituation phase, the animal had free access to all chambers for 10 min. After this session, two identical small cages (15 cm x 8 cm x 10 cm) were placed in each end-chamber. A novel conspecific (i.e., BALB/cJ male mouse of the same age as the experimental mouse) was placed into one of the two small cages ('social chamber') while the other cage remained empty. In this sociability phase, the experimental mouse was then allowed to explore the apparatus for 10 min. In the last session (the preference for social novelty phase), a second unfamiliar mouse was placed in the previously empty cage ('novel chamber'), while the now familiar conspecific remained in its original cage ('familiar chamber'). The experimental mouse was then allowed to explore the entire apparatus for another 10 min. During all phases, time spent in each of the three chambers was measured. Preference for social novelty was determined by calculating the ratio of the time spent in the 'novel chamber' *versus* the 'familiar chamber' in the third session. The SNP test was performed over three days (days #59, 60 and 61) due to the duration of the test (30 min per animal); mice were randomly distributed into the three day batches.

**Resident-intruder test (RI).** Agonistic (social aggression) behavior was assessed by the RI test on day #57 (1). An 'intruder' mouse (A/J male mouse characterized by low aggressiveness (17)) was introduced in the home cage of the 'resident' mouse. The aggressiveness of the resident was measured by the latency of the first attack and the number of attack(s) over a 5-min period (mean  $\pm$  SEM for the number of attack(s): control group  $1.11 \pm 0.56$ , UCMS group  $5.00 \pm 0.71$ ). The latency and frequency of the resident's mounting behavior were also recorded. No attacks by intruders were observed.

**Novelty-suppressed feeding test (NSF).** The NSF test to assess anxiety behavior was performed as previously described (2). Twelve hours before the test, mice were fasted by removing food from their cages. At the time of testing (day #47), a single pellet of food (regular chow) was placed on a white paper positioned in the center of a square open-field (33 x 33 x 30 cm) the floor of which was covered with sawdust. The mouse was placed at one of the corner of the open-field, and the latency to chew the pellet was recorded during 3-min. This test is based on the conflict between the drive to eat the food pellet and venturing into a novel environment.

**Forced swim test (FST).** Behavioral despair was assessed on day #44 using a modified version of the FST previously described (18). Mice were placed for six minutes into a glass cylinder (diameter: 17.5 cm; Height: 25 cm) filled with 15 cm of water (24°C). This test allows assessment of the resignation (behavioral despair) measured by the duration of immobility, recorded during the last four minutes of the test. A mouse was considered immobile when floating passively performing only slight movements of its limbs and tail. The 'immobility' included slow drifting on the water surface without any initiation of swimming. Two mice ( $n = 1$  per group) were excluded from the analysis as they displayed difficulties to maintain their head above the water and the test was immediately terminated.

**The reward-driven exploratory test (RDE).** This test (also known as 'cookie test') was designed (5) to evaluate anhedonia-like behavior by assessing the exploration of a three-chambered maze to collect a palatable stimulus over four sessions. It was conducted in a custom-made apparatus consisting of three aligned compartments of the same dimension (20x20x20 cm) of different colors (i.e., white, grey and black). The three compartments are connected by two gates controlled by the experimenters. Mice were familiarized with a piece of chocolate biscuit (McVitie's Digestives with dark chocolate,  $2 \pm 0.5$  g (Mean  $\pm$  SD) three days a week during three weeks (week #2: days #10, 12 and 14; week #3: days #17, 19 and 21; week #4: days #24, 26 and 28). The two weeks before the first session were 'biscuit-free'. One hour before testing, the food was removed from the cage lid in order to avoid inter-individual differences in the drive for food. Each session lasted five minutes. A piece of biscuit (approximately 2g) was placed at the center of the black (third) compartment. The mouse was placed in the white (first) compartment of the apparatus, the head facing the opposite side to the gate. The gate between the 2 first compartments was placed after the

mouse entered the second grey compartment. Entry into the second compartment took place within two minutes (the mouse was gently guided if required). During each session, the latency to cross the first and the second gate, the latency to smell and to chew the biscuit, as well as biscuit consumption (i.e., number of bites), were recorded. The four test sessions were performed within ten days with an inter-test interval of two days (days #43, 46, 49, and 52).

### **Brain tissue and blood collection**

At the end of the protocol, mice were euthanized between ZT12.5 and ZT14.5. and the prefrontal cortex, the hippocampus and the hypothalamus were collected as previously described (19). Brain tissues were immediately immersed in RNAlater® (Sigma-Aldrich, St. Louis, MO, USA) and stored at -20°C until use, while trunk blood was collected in RNAProtect Animal Blood tubes (76544; Qiagen, Hilden, Germany).

### **RNA Extraction**

Total RNA was extracted from dissected brain tissue using the RNeasy® Fibrous Tissue Mini Kit (Qiagen, Hilden, Germany), following the manufacturer's instructions. Total RNA was extracted from whole blood samples using the RNeasy® Protect Animal Blood Kit (Qiagen, Hilden, Germany). RNA samples were assessed for quantity and integrity (RNA Integrity Number: brain samples,  $9.95 \pm 0.02$ ; blood samples,  $7.95 \pm 0.15$ ) using the NanoDrop 8000 spectrophotometer V2.0 (ThermoScientific, Wilmington, DE, USA) and Agilent 2100 Bioanalyser (Agilent Technologies, Waldbronn, Germany), respectively.

### **Library generation and sequencing**

Total RNA libraries were prepared using 100 ng of total RNA from each sample, the NEBNext® rRNA Depletion Kit and the NEBNext® Ultra Directional RNA library preparation kit. Fragmentation prior to first strand cDNA synthesis was carried out using incubation conditions recommended by the manufacturer for samples with a RIN > 7 (94°C for 15 minutes), and 15 cycles of PCR were performed for final library enrichment. Resulting libraries were quantified using the Qubit 2.0 spectrophotometer (Life Technologies, Carlsbad, CA, USA) and average fragment size assessed using the Agilent 2200 TapeStation (Agilent Technologies, Waldbronn, Germany). Sample libraries with compatible index sequences were pooled together, resulting in two separate pools of tissue-derived libraries each containing 24 samples, and one blood-derived library with all 16 samples. One-hundred base pair paired-end reads were generated for each library using the Illumina HiSeq®2500 (Illumina Inc., San Diego, CA, USA). At least 40 million reads were obtained for brain tissue samples, whereas for the blood samples a minimum of 60 million reads was obtained.

### **Gene expression profiling**

Quality control (QC) of sequencing reads, read alignment and feature quantification were performed using a RNA sequencing workflow developed by Eli Lilly and Company. Briefly, FASTQ files were first checked for integrity and potential transfer errors prior to QC. QC was performed on both pre-aligned reads (base quality, base composition, heterologous organisms, rRNA/mitochondrial/viral and adaptor content) and post-alignment. In the first instance, location type count summary, template length, species, DNA genotype/RNA genotype match, sample relatedness/intermixing, and 3'-bias were assessed. No samples were excluded from the alignment analysis based on these QC measures. Alignment of reads against the genome of the *Mus musculus* strain C57BL/6J (assembly GRCm38.p4) was performed with GSNPA (20). Feature quantification was performed at the exon level and a counting algorithm using the NCBI-based gene models.

Exons defined by these gene models served as the base feature to which counts are attributed. Count data were subsequently normalized at the gene level. Different methods for data normalization were explored. Of the methods applied, Robust Linear Model (RLM) and quartile normalization (75% quartile; QM) were chosen following visual inspection of the distribution curves. Summary statistics (minimum value, 1<sup>st</sup> quartile, median, mean, 3<sup>rd</sup> quartile and maximum value) for each normalized sample were generated. Kernel density plots were applied to visualize the underlying distribution of all variables within our data and median values were visualized using boxplots to examine the variability between samples within each tissue. Principle Component Analysis (PCA) plots were inspected to examine the variability and clustering of each biological sample both within each tissue and across all tissues. Each tissue type was plotted by hierarchical clustering analysis to determine their relationship by similarity (Euclidean distance) to each other. Trees were within 0.2 apart. Following QC, normalization and descriptive statistics, all samples were carried forward for differential expression analysis.

### **Rank Products analysis for DEG identification**

Differential expression analysis between control and UCMS-subjected animals was performed using the non-parametric Rank Product statistical method that is independent of inter-class variability (21, 22), using the R Bioconductor package RankProd (23). Significance was set at a proportion of false positive (FP; abbreviated  $P_{fp}$  in the text)  $< 0.05$ .

A PubMed search (<https://www.ncbi.nlm.nih.gov/pubmed>) was performed (August-September 2017) to determine the putative involvement of each DEG in stress response (search term: 'stress'), sleep (search terms: 'sleep' and/or 'circadian'), neuropsychiatric symptoms (e.g., 'depression', 'depressive', 'eating', 'weight', anxiety', 'aggressiveness', 'social', 'reward'), mood disorders (e.g., 'depression', 'depressive', 'mood', 'affective') and neurodegenerative diseases ('Alzheimer', 'Parkinson', 'dementia'). Associations with each of the above categories were color-coded and reported (Fig. S6A and *SI Appendix*, Dataset S3).

### **Selecting genes associated with a given phenotype**

Since in our data set, as is the case in most -omics data sets, there are many more potential predictors than observations, special statistical methods to robustly select relevant predictors need to be used. We used a form of penalized regression which is referred to as Elastic-net.

By penalizing the magnitude and/or number of coefficient estimates of all features, Elastic Net (24) is able to produce a regression model without overfitting to the data, with only a slight increase in bias (i.e., under-fitting of data or not identifying relevant predictors). For transcriptomic data, where the number of features is greater than the number of samples, such approaches are critical for reducing the complexity of the overall model whilst maintaining high prediction accuracy (25). Elastic-net is a hybrid of Ridge (26) and LASSO (27) regression as it combines the different penalties employed by each approach (L2 norm and L1 norm respectively). Combining penalties enables the generation of sparse, parsimonious models (models where coefficients can equal 0, to select for the most relevant features, as per LASSO), whilst allowing for all correlated features, such as those targeting transcripts encoding proteins involved in the same pathway/biological process, to appear in the model (as per Ridge regression) (24), in keeping with our overall aim.

All Elastic-net learning was performed using the R package glmnet (28). There are two hyper-parameters that influence Elastic-net learning; alpha, which controls the balance of LASSO-like and Ridge-like penalties, and lambda, which controls the overall strength of the penalties to apply (where greater lambda values reduces the number of genes selected, as well as their coefficients). Here we fixed alpha at 0.5, to equally balance the penalties. To identify the optimal value of lambda for a given attribute (label) we performed an exhaustive grid search of all possible leave-2-samples-

out combinations of the labelled data set and lambda values in the range of 0-5 with an increment of 0.01. Here, two samples (one from the UCMS group and one from the control group) were used to independently assess the accuracy (Mean squared Error, MSE) of the predictions made by the regression model trained on all other samples under the constraints of the penalties dictated by the given lambda value. Subsequently, the value of lambda that produced the minimum MSE across all possible leave-two-out combinations was selected as the optimal value of lambda for that label. Using this optimal value of lambda as input to the glmnet function, a final predictive model, trained on all samples, was produced for the given label. Genes (features) with a non-zero coefficient in the final predictive model were defined as genes associated with the label (phenotype). Where the optimal lambda value produced a model comprising no genes (i.e. only the intercept is a parameter in the final predictive model) then the next lowest lambda value giving the minimum MSE across all leave-two-out combinations was used to generate a list of genes associated with the label/variable. We conducted these analyses focusing on sleep variables, three behavioural variables and HPA axis response, the values of which were z-scored within group in order to identify associations with phenotypes independent of any 'unspecific' group effect. We only report predictor sets for variables achieving a positive Pearson correlation  $r$  between observed and cross-validated prediction values  $> 0.31$ .

### **Functional annotation and interpretation**

Generic functional information for proteins encoded by DEGs or predictors were obtained, and last updated in June 2018, using GeneCards (<https://www.genecards.org/>) and the reviewed knowledgebase resources of UniProt using GeneID (Entrez Gene) (UniProtKB\_Swiss-Prot; <http://www.uniprot.org/>). Lists of genes associated with an attribute, either by Rank Products analysis or Elastic-net learning, were subjected to Gene Ontology (GO) enrichment analyses using the software GeneGo (Gene Ontology (GO) processes; and/or Pathway maps in MetaCore™ (GeneGo, Thomson Reuters; <https://portal.genego.com/>; updated June 2018). Significant enrichment was defined by nominal  $P$ -value ( $P_{\text{nom}}$ )  $< 0.05$  and False Discovery Rate-adjusted  $P$  ( $P_{\text{adj}}$ )  $< 0.05$ .

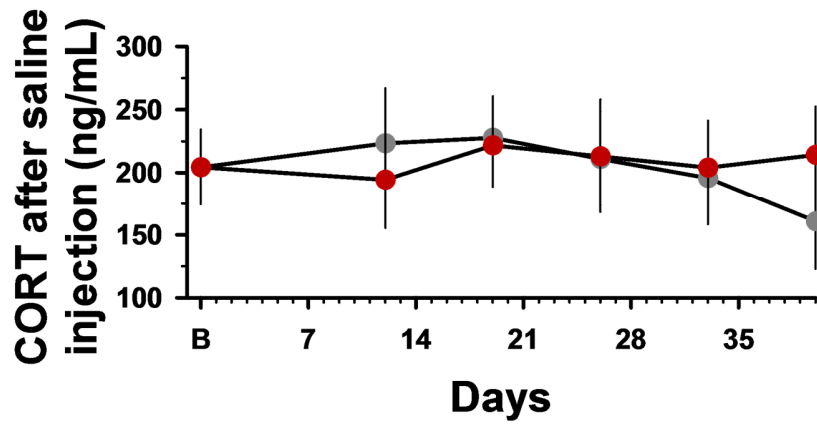
### **Similarity of gene lists associated with a variable across tissues**

To assess the similarity of gene lists associated with a given variable across tissues the intersection and set differences of each list were generated. The significance of an observed intersection set formed from the comparison of different lists was calculated using a Z-test, comparing the size of the observed intersection set with a background distribution of intersection set sizes. The background distribution for a given comparison was generated by generating random lists of genes (selected from the total set of genes across tissues), the same number and size of those being compared in the true lists being compared, and calculating set sizes, repeated 10,000 times.

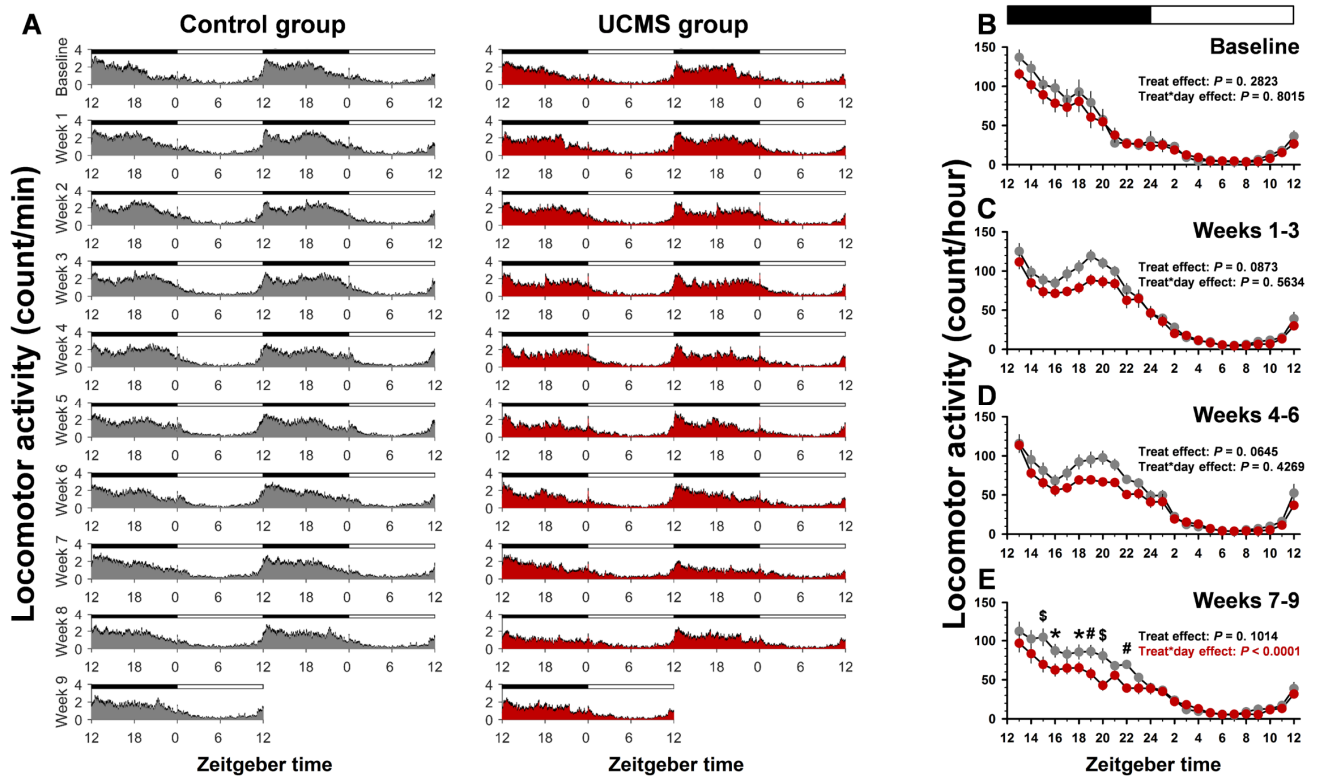
### **Similarity of gene lists between variables within a tissue**

To determine the significance of an observed overlap between two lists of genes for two given variables within a tissue we used the hypergeometric test (phyper function in R) to generate a 'raw' nominal  $P$ -value ( $P_{\text{nom}}$ ). The resultant  $P$ -value was based on the observed overlap between the two gene lists, the size of each gene list, and the size of the tissue-specific transcriptome as background. All raw  $P$ -values within a tissue were adjusted (abbreviated to  $P_{\text{adj}}$  in the text) using the Benjamini and Hochberg false discovery rate correction (p.adjust function in R).

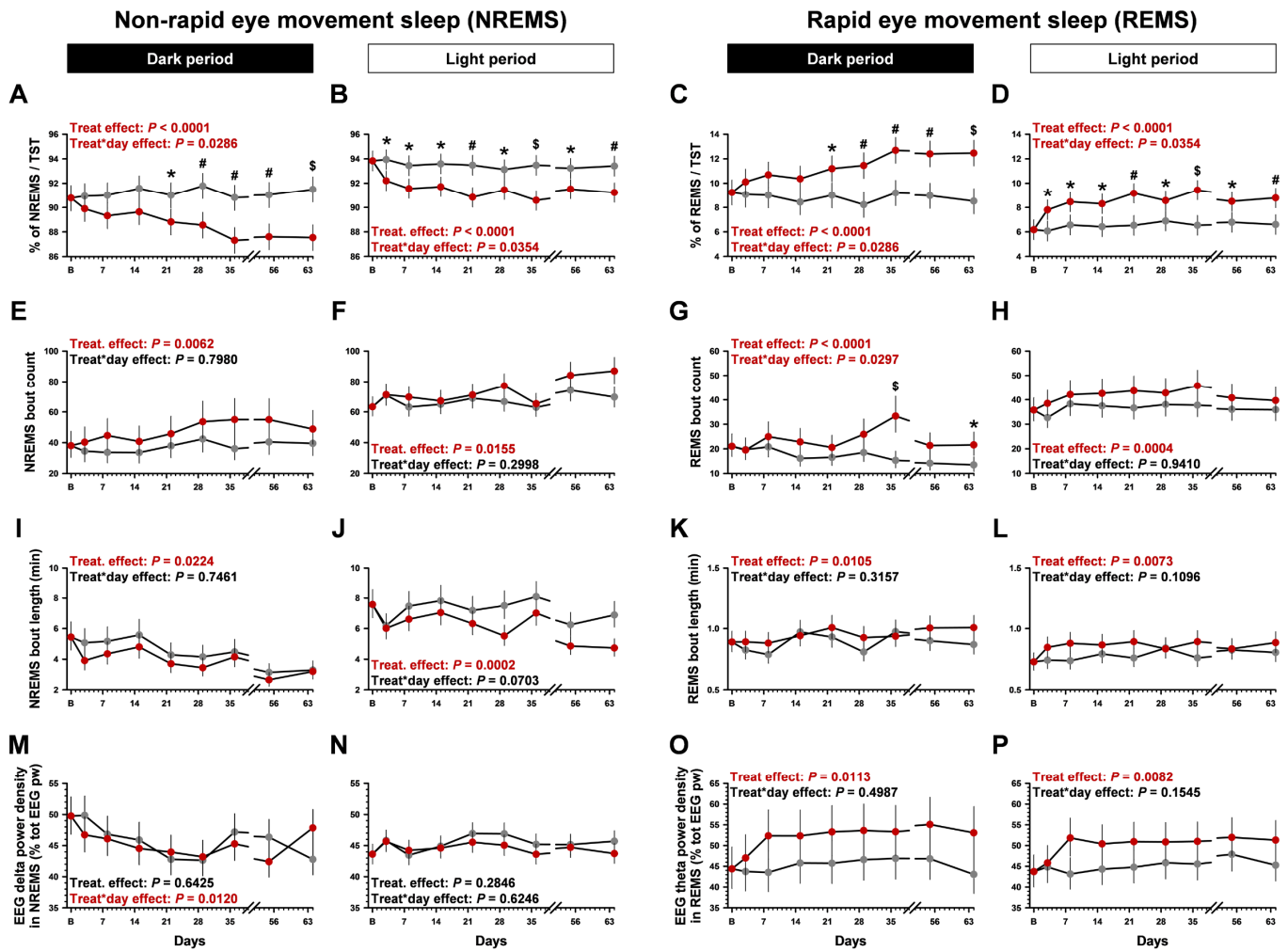




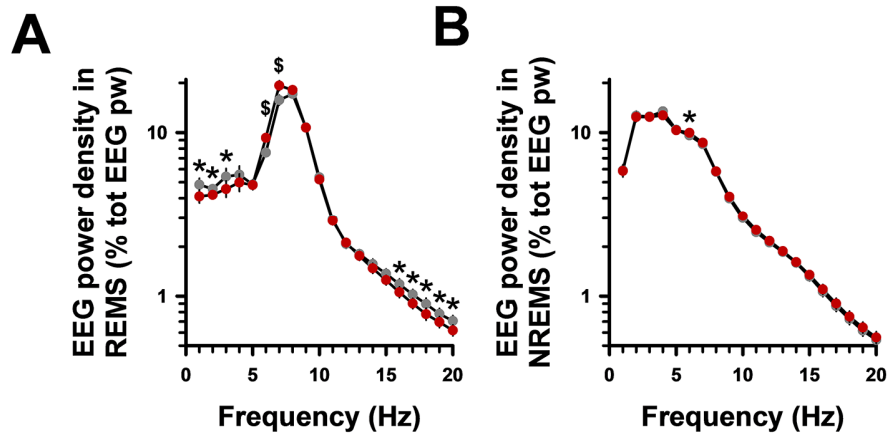
**Fig. S1. Corticosterone levels following saline injection in the dexamethasone (DEX) suppression test.** No effect of ‘treatment’ ( $P = 0.6573$ ), nor ‘treatment’ x ‘day’ interaction ( $P = 0.4642$ ), was observed in general linear mixed model. Data are Least Square Means  $\pm$  95% Confidence Intervals (controls: grey; UCMS: red;  $n = 5-7$  per group). For detailed statistics, see *SI Appendix*, Datasets S1.



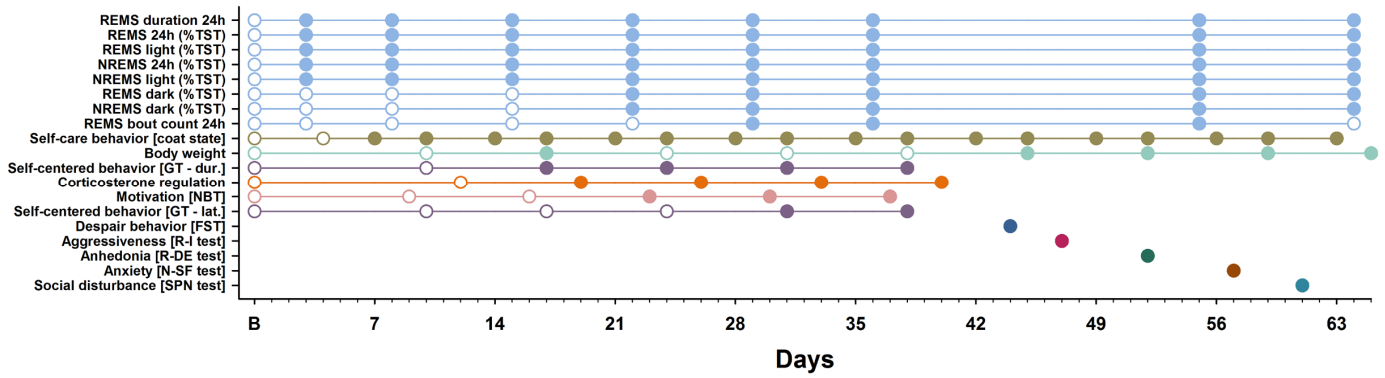
**Fig. S2. 24-h rest-activity rhythms averaged per week.** Rest-activity rhythms were continuously monitored throughout the ten-week experiment including baseline and the nine-week UCMS paradigm. (A) Double-plotted 24-h locomotor activity counts summed by one-minute intervals (grey or red for control or UCMS group respectively: Mean; black: SEM;  $n = 9$  per group). (B-E) 24-h locomotor activity counts summed by one-hour intervals for (B) baseline, (C) averaged weeks 1 to 3, (D) averaged weeks 4 to 6 and (E) averaged weeks 7 to 9. Data are Mean  $\pm$  SEM (controls: grey; UCMS: red;  $n = 9$  per group). Light OFF at Zeitgeber time (ZT) 12 and light ON at ZT0; \* $P < 0.05$ , # $P < 0.01$ ,  $^{\$}P < 0.001$  (*post-hoc* comparisons for (B-E) significant ‘treatment’ x ‘ZT’ interaction in general linear mixed model). For detailed statistics, see *SI Appendix*, Datasets S1.



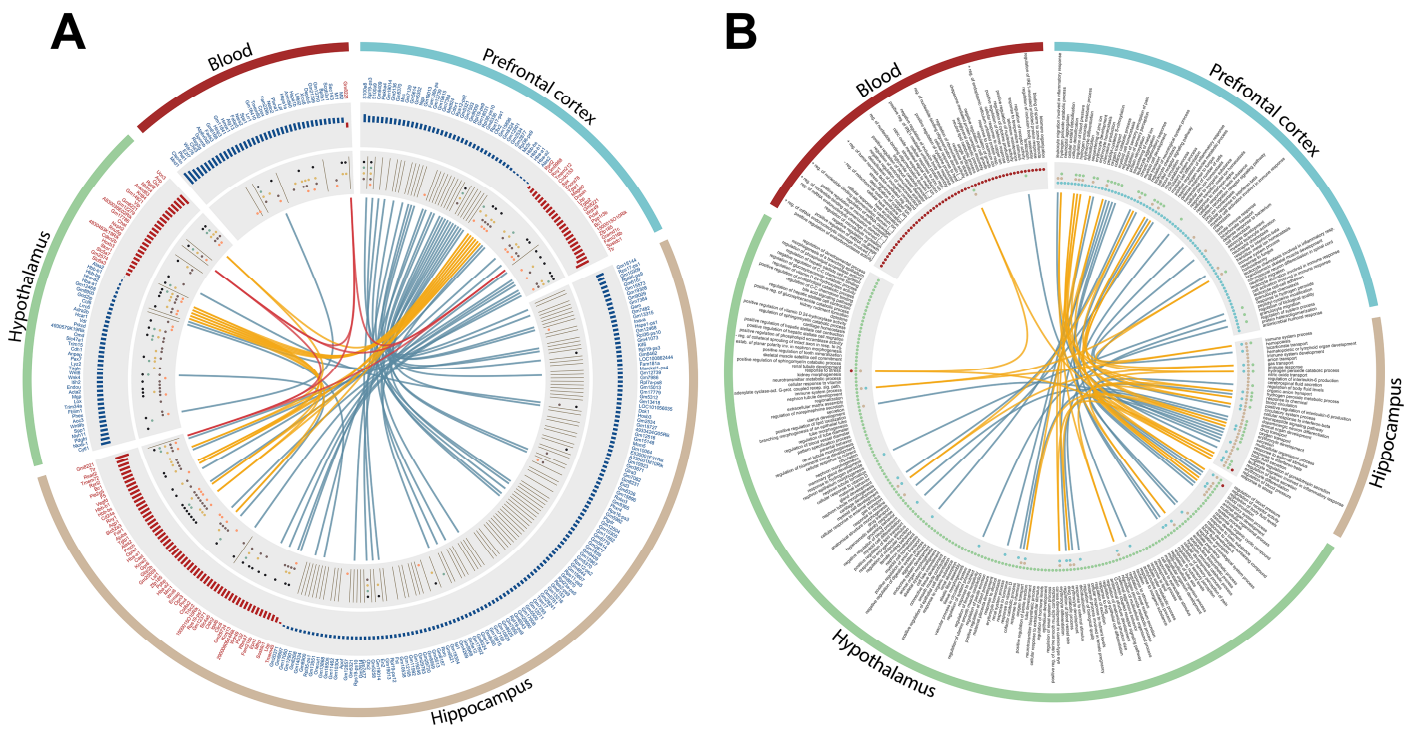
**Fig. S3. Time-course of UCMS-induced alterations on sleep and the electroencephalogram (EEG) during the dark and light phases.** (A-D) Time spent in non-rapid eye movement sleep (NREMS) and rapid eye movement sleep (REMS) as percentage of total sleep time (TST) during the dark and light phases. (E-H) Number and (I-L) duration of sleep episodes. (M-N) EEG delta (1-4.5 Hz) power density in NREMS and (O-P) EEG theta (6-9 Hz) power density in REMS during the dark and light phases. Least Square Means  $\pm$  95% Confidence Intervals (controls: grey; UCMS: red;  $n = 8$  per group); \*  $P < 0.05$ , #  $P < 0.01$ , \$  $P < 0.001$  (*post-hoc* comparisons for significant ‘treatment’ x ‘day’ interaction in general linear mixed model). For detailed statistics, see *SI Appendix*, Datasets S1.



**Fig. S4. Electroencephalogram (EEG) power density.** Relative EEG power spectra in (A) rapid eye movement sleep (REMS) and (B) non-rapid eye movement sleep (NREMS) during the 12-h light phase (averaged spectra of all EEG recording sessions during the 9-week UCMS protocol). Data are Least Square Means  $\pm$  95% Confidence Intervals (controls: grey; UCMS: red;  $n = 8$  per group); \* $P < 0.05$ , § $P < 0.001$  (effect of ‘treatment’ in general linear mixed model). pw: power; tot: total. For detailed statistics, see *SI Appendix*, Datasets S1.



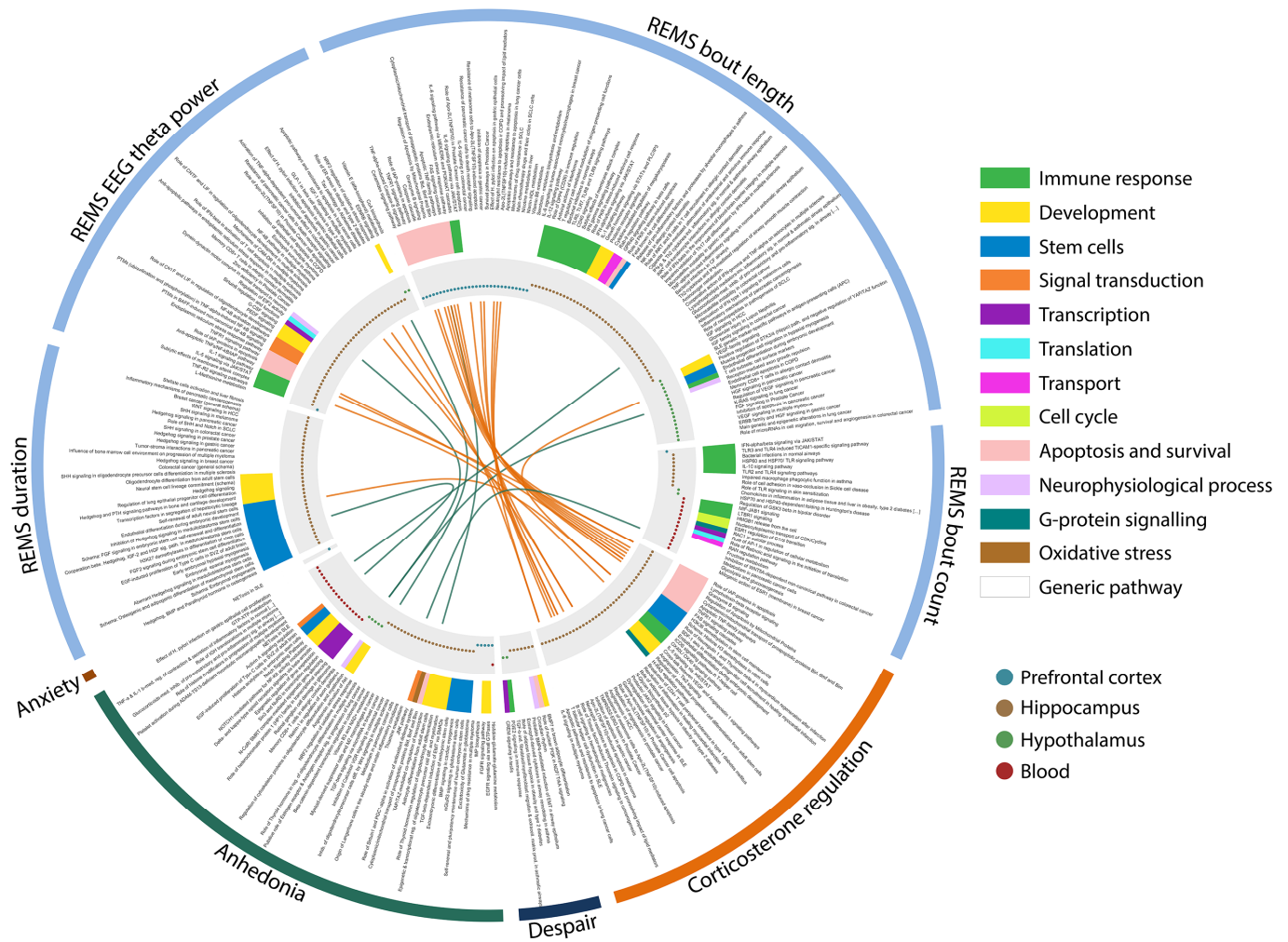
**Fig. S5. Temporal emergence of UCMS-induced physical, behavioral, neuroendocrine, neurochemical and sleep-related symptoms.** Schematic representation of the emergence of physical, endocrine, behavioral, electrophysiological measures during the UCMS paradigm. Circles indicate days on which parameters were assessed, and open and filled circles correspond respectively to non-significant and significant differences between the UCMS and control groups.



**Fig. S6. Characterization and functional enrichment of genes differentially expressed following chronic mild stress in different tissues.** (A) Differentially expressed genes. The various tracks/circles indicate the following. Outer track: tissue. Second track: gene names (blue: upregulated genes; red: downregulated genes;  $P_{\text{PIP}} < 0.05$ ). Third track: length of blue and red bars indicate  $\log_2$  fold-change of the DEGs. Innermost grey track: the dots refer to conditions in which the DEGs have been reported as being associated with/implicated in (conditions: stress response [brown], sleep [orange], behavioral and neurobiological changes corresponding to human ‘neuropsychiatric’ symptoms [ochre], mood disorders [green] and neurodegenerative diseases [black]; for details and references, see *SI Appendix*, Datasets S3). The grey lines in the innermost grey track indicate processed pseudogenes. The arcs in the center circle depict the overlap between tissues (blue arc: two tissues; yellow arc: three tissues; red arc: four tissues). (B) Significantly enriched Gene Ontology (GO) biological processes for differentially expressed genes (DEGs) in the prefrontal cortex, hippocampus, hypothalamus and whole blood, after nine-week unpredictable chronic mild stress. Enrichment analyses were performed using MetaCore™ ‘GO Processes’ (GeneGo, Thomson Reuters; <https://portal.genego.com/>) and significance was set at FDR adjusted  $P$ -value ( $P_{\text{adj}}$ )  $< 0.05$ . The various tracks/circles indicate the following. Outer track: tissue. Second track: processes names. Third track: tissues in which biological processes were found to be significantly enriched (blue: prefrontal cortex; brown: hippocampus; green: hypothalamus; red: blood). Overlaps between the different tissues are illustrated by arcs in the inner circular track (blue: overlap between two tissues; yellow: overlap between three tissues).  $n = 8$  per group for brain regions;  $n = 7$  controls *versus*  $n = 9$  UCMS group for blood. This information is available in tabular format (see *SI Appendix*, Datasets S4).

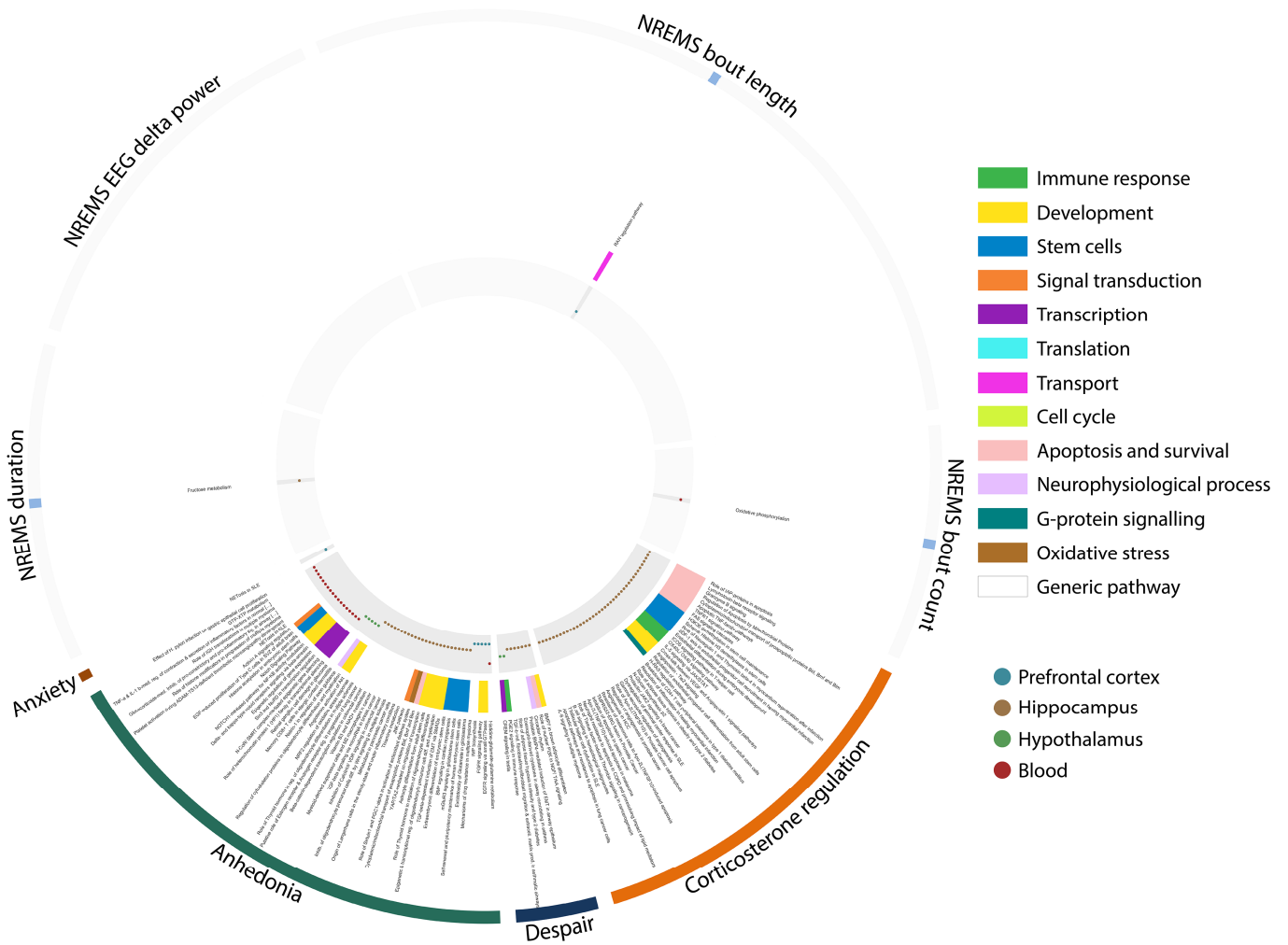


**Fig. S7. Pathways associated with the transcriptome response to chronic mild stress in different tissues.** Significantly enriched biological pathways for differentially expressed genes (DEGs) in the prefrontal cortex, hippocampus, hypothalamus and whole blood, after nine-week unpredictable chronic mild stress. Enrichment analyses were performed using MetaCore™ ‘Pathway Maps’ tool (GeneGo, Thomson Reuters; <https://portal.genego.com/>) and significance was set at FDR adjusted  $P$ -value ( $P_{adj}$ ) < 0.05. The various tracks/circles indicate the following. Outer track: tissue. Second track: pathway names. Third track: functional themes of pathways.  $n = 8$  per group for brain regions;  $n = 7$  controls *versus*  $n = 9$  UCMS group for blood. This information is available in tabular format (see *SI Appendix*, Datasets S4).








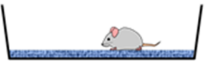


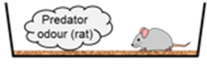
**Fig. S8. Enriched pathways associated with transcriptomic predictors of sleep, corticosterone regulation and behavioral variables.** Enriched REMS- (top) and behavioral/neuroendocrine (bottom) associated pathways. Tracks from outside-in, outer track: phenotypes; second track: significantly enriched pathways (identified using the ‘Pathway Maps’ tool in MetaCore™, Thomson Reuters; <https://portal.genego.com/>); third track: functional themes of enriched pathways; fourth track: tissues in which pathways were found to be significantly enriched (blue: prefrontal cortex; brown: hippocampus; green: hypothalamus; red: blood). Overlaps between pathways are illustrated by arcs in the inner circular track, which color corresponds to behavioral/neuroendocrine phenotypes. All depicted pathways were significant at FDR adjusted  $P$ -value ( $P_{adj}$ ) < 0.05;  $n = 8$  per group for brain regions;  $n = 7$  controls versus  $n = 9$  UCMS group for blood. This information is available in tabular format (see *SI Appendix*, Datasets S9).





**Fig. S9. Enriched pathways associated with transcriptomic predictors for NREMS, behavioral and neuroendocrine variables.** Enriched NREMS- (top) and behavioral/neuroendocrine (bottom) associated pathways. Tracks from outside-in, outer track: phenotypes; second track: significantly enriched pathways (as identified using the ‘Pathway Maps’ tool in MetaCore™, Thomson Reuters; <https://portal.genego.com/>); third track: functional themes of enriched pathways; fourth track: tissues in which pathways were found to be significantly enriched (blue: prefrontal cortex; brown: hippocampus; green: hypothalamus; red: blood). Overlaps between pathways are illustrated by arcs in the inner circular track (no overlap was observed). All depicted pathways were significant at FDR adjusted  $P$ -value ( $P_{adj}$ ) < 0.05;  $n = 8$  per group for brain regions;  $n = 7$  controls versus  $n = 9$  UCMS group for blood. This information is available in tabular format (see *SI Appendix, Datasets S9*).

**Table S1. List of socio-environmental stressors used for the unpredictable chronic mild stress paradigm (UCMS)**

Stressor	Description	Illustration
Social stress	Each mouse is placed in an empty cage previously occupied by another individual	
Cage tilting	Cages are tilt backwards (45°) during 1 to 4 hours	
Confinement stress	Mice are kept in closed and ventilated tubes for 30 to 60 min (they can turn themselves back into the tube)	
Without sawdust	The sawdust is removed during 2 to 24 hours	
Soiled sawdust	The clean sawdust is replaced by soiled sawdust coming from control mice	
Damp sawdust	Animal sawdust is soaked in water for 2 to 12 hours	
Sawdust change	The sawdust is changed three times every 30 min or every hours	
Water stress	The sawdust of each cage is removed and replaced by water (about 1 cm of water at 20°C) for 30 to 60 min	
Predator odor	Rat sawdust (with feces) is deposited in each cage for a period of 1 to 2 hours	

Two socio-environmental mild stressors are randomly applied each day during the dark period, throughout the UCMS paradigm, except during sleep EEG/EMG recordings.

**Datasets S1 (separate file). *P*-values, Cohen's  $f^2$  and Intra-class correlations (ICC) associated with data displayed in Figs. 1, 2, S1, S2, S3 and S4.** *P*-values (overall effect of 'treatment', 'day', treatment\*day interaction and between-group contrasts) were computed using a general linear mixed model with baseline as covariate when appropriate. To assess statistical effect sizes, Cohen's  $f^2$  were computed. ICC were calculated to assess variability.

**Datasets S2 (separate file). Bivariate correlations across physical, behavioral, sleep and neuroendocrine and sleep parameters.** Kendall's Tau partial correlation coefficients and associated *P*-values and FDR adjusted *P*-values between pairs of symptoms induced by UCMS. The effect of 'group' was controlled (i.e., control *versus* UCMS) to identify bivariate associations at the level of the individual independent of 'unspecific' group effects.

**Datasets S3 (separate file). UCMS-induced differentially expressed genes (DEGs) in the prefrontal cortex, hippocampus, hypothalamus and blood.** DEGs were identified using the non-parametric Rank Product statistical method. Computed Rank Product statistic (RP/Rsum), log<sub>2</sub> transformed fold-change (Log2FC), proportion of false positive (PFP), *P*-value, overlap with other tissues, and their involvement(s) in sleep/circadian rhythms (studies in humans and animals), stress response (studies in animals), behavioral and neurobiological changes corresponding to human 'neuropsychiatric' symptoms (NPS; studies in humans and animals), mood disorders (MD; human studies) and neurodegenerative diseases (NDD; studies in humans and animals) [PMID of references are provided] are listed.

**Datasets S4 (separate file). Enrichment analyses of the UCMS-induced differentially expressed genes (DEGs) in the prefrontal cortex, hippocampus, hypothalamus and blood.** Gene Ontology (GO) biological processes and pathways associated with the DEGs between control and stressed mice after the nine-week unpredictable chronic mild stress paradigm. Processes and pathways were identified using the 'GO Processes' and 'Pathway Maps' tools in MetaCore™ (GeneGo, Thomson Reuters; <https://portal.genego.com/>). Significantly enriched processes (FDR adjusted *P*-value < 0.05) are indicated in bold.

**Datasets S5 (separate file). Bivariate correlations between differentially expressed genes (DEGs) and physical, behavioral, neuroendocrine and sleep parameters.** Kendall's Tau partial correlation coefficients and associated *P*-values and FDR adjusted *P*-values between DEGs (prefrontal cortex, hippocampus, hypothalamus and blood) and physical, behavioral, neuroendocrine and sleep variables.

**Datasets S6 (separate file). Transcriptomic predictors (features) of phenotypic variables (labels) identified using elastic-net learning.** Number of predictors for selected labels are displayed, as well as raw coefficient values between predictors and labels.

**Datasets S7 (separate file). Overlap between sets of transcriptomic predictors for REMS, NREMS, neuroendocrine and behavioral phenotypes.** Number of overlap(s) and associated *P*-values and FDR adjusted *P*-values. Significance of overlaps between sets of transcriptomic predictors, identified using the Elastic-net approach, for REMS, NREMS, neuroendocrine and behavioral phenotypes in the prefrontal cortex, hippocampus, hypothalamus and the blood, were computed using a hypergeometric test. *P*-values were adjusted for multiple comparisons with the Benjamini-Hochberg procedure. Pink squares indicate significant overlap with FDR adjusted *P* < 0.05.

**Datasets S8 (separate file). List of transcriptomic predictors of sleep, behavioral and endocrine phenotypes, previously implicated in the regulation of sleep and/or circadian**

**rhythms, neural transmission, immune system, mitochondrial function, as well as psychiatric disorders.**

**Datasets S9 (separate file). List of enriched pathways associated with transcriptomic features predicting sleep, behavioral and neuroendocrine phenotypes.** Transcriptomic features were identified by the Elastic-net approach in the three brain regions and blood after the nine-week UCMS paradigm. Biological pathways associated with identified features were determined using the 'Pathway Maps' tool in MetaCore™ (GeneGo, Thomson Reuters; <https://portal.genego.com/>).

## References

1. Nollet M, *et al.* (2011) Activation of orexin neurons in dorsomedial/perifornical hypothalamus and antidepressant reversal in a rodent model of depression. *Neuropharmacology* 61(1-2):336-346.
2. Nollet M, *et al.* (2012) Neurogenesis-independent antidepressant-like effects on behavior and stress axis response of a dual orexin receptor antagonist in a rodent model of depression. *Neuropsychopharmacology* 37(10):2210-2221.
3. Hasan S, van der Veen DR, Winsky-Sommerer R, Dijk DJ, & Archer SN (2011) Altered sleep and behavioral activity phenotypes in PER3-deficient mice. *Am J Physiol Regul Integr Comp Physiol* 301(6):R1821-1830.
4. Willner P (2017) The chronic mild stress (CMS) model of depression: History, evaluation and usage. *Neurobiol Stress* 6:78-93.
5. Nollet M, Le Guisquet AM, & Belzung C (2013) Models of depression: unpredictable chronic mild stress in mice. *Curr Protoc Pharmacol* Chapter 5:Unit 5 65.
6. Belzung C & Griebel G (2001) Measuring normal and pathological anxiety-like behaviour in mice: a review. *Behav Brain Res* 125(1-2):141-149.
7. Vogt MA, *et al.* (2017) May the use of different background strains 'strain' the stress-related phenotype of GR(+/-) mice? *Behav Brain Res* 335:71-79.
8. Ibarguen-Vargas Y, Surget A, Touma C, Palme R, & Belzung C (2008) Multifaceted strain-specific effects in a mouse model of depression and of antidepressant reversal. *Psychoneuroendocrinology* 33(10):1357-1368.
9. Yalcin I, Belzung C, & Surget A (2008) Mouse strain differences in the unpredictable chronic mild stress: a four-antidepressant survey. *Behav Brain Res* 193(1):140-143.
10. Gosselin T, *et al.* (2017) Fluoxetine induces paradoxical effects in C57BL6/J mice: comparison with BALB/c mice. *Behav Pharmacol* 28(6):466-476.
11. Ohkura N, *et al.* (2007) Comparative study of circadian variation in numbers of peripheral blood cells among mouse strains: unique feature of C3H/HeN mice. *Biol Pharm Bull* 30(6):1177-1180.
12. Golde WT, Gollobin P, & Rodriguez LL (2005) A rapid, simple, and humane method for submandibular bleeding of mice using a lancet. *Lab Anim (NY)* 34(9):39-43.
13. Van Gelder RN, Edgar DM, & Dement WC (1991) Real-time automated sleep scoring: validation of a microcomputer-based system for mice. *Sleep* 14(1):48-55.
14. McCarthy A, *et al.* (2016) REM sleep homeostasis in the absence of REM sleep: Effects of antidepressants. *Neuropharmacology* 108:415-425.
15. Deacon RM (2006) Assessing nest building in mice. *Nat Protoc* 1(3):1117-1119.
16. Moy SS, *et al.* (2004) Sociability and preference for social novelty in five inbred strains: an approach to assess autistic-like behavior in mice. *Genes Brain Behav* 3(5):287-302.
17. Dow HC, *et al.* (2011) Genetic dissection of intermale aggressive behavior in BALB/cJ and A/J mice. *Genes Brain Behav* 10(1):57-68.
18. Petit-Demouliere B, Chenu F, & Bourin M (2005) Forced swimming test in mice: a review of antidepressant activity. *Psychopharmacology (Berl)* 177(3):245-255.

19. Spijker S (2011) Dissection of Rodent Brain Regions. *Neuromethods*, ed Li KW), Vol 57, pp 13-26.
20. Wu TD & Nacu S (2010) Fast and SNP-tolerant detection of complex variants and splicing in short reads. *Bioinformatics* 26(7):873-881.
21. Breitling R, Armengaud P, Amtmann A, & Herzyk P (2004) Rank products: a simple, yet powerful, new method to detect differentially regulated genes in replicated microarray experiments. *FEBS Lett* 573(1-3):83-92.
22. Magistri M, Velmeshev D, Makhmutova M, & Faghihi MA (2015) Transcriptomics Profiling of Alzheimer's Disease Reveal Neurovascular Defects, Altered Amyloid-beta Homeostasis, and Deregulated Expression of Long Noncoding RNAs. *J Alzheimers Dis* 48(3):647-665.
23. Hong F, *et al.* (2006) RankProd: a bioconductor package for detecting differentially expressed genes in meta-analysis. *Bioinformatics* 22(22):2825-2827.
24. Zou H & Hastie T (2005) Regularization and variable selection via the elastic net. *J Roy Stat Soc B* 67:301-320.
25. James G, Witten D, Hastie T, & Tibshirani R (2013) *An introduction to statistical learning : with applications in R* (Springer, New York) pp xvi, 426 pages.
26. Hoerl AE & Kennard RW (1970) Ridge Regression - Applications to Nonorthogonal Problems. *Technometrics* 12(1):69-&.
27. Tibshirani R (1996) Regression shrinkage and selection via the Lasso. *J Roy Stat Soc B Met* 58(1):267-288.
28. Friedman J, Hastie T, & Tibshirani R (2010) Regularization Paths for Generalized Linear Models via Coordinate Descent. *J Stat Softw* 33(1):1-22.